Palaeogeography, Palaeoclimatology, Palaeoecology 466 (2017) 202–208

Contents lists available at ScienceDirect

Palaeogeography, Palaeoclimatology, Palaeoecology

journal homepage: www.elsevier.com/locate/palaeo

Zinc and cadmium stable isotopes in the geological record: A case study from the post-snowball Earth Nuccaleena cap dolostone

Seth G. John [a,*], Marcus Kunzmann [b,c], Emily J. Townsend [d], Angela D. Rosenberg [d]

[a] Department of Earth Sciences, University of Southern California, Los Angeles, CA, USA
[b] CSIRO Mineral Resources, Australian Resources Research Centre, Kensington, WA 6151, Australia
[c] Northern Territory Geological Survey, Darwin, NT 0800, Australia
[d] Department of Earth and Ocean Sciences, University of South Carolina, Columbia, SC, USA

ARTICLE INFO

Article history:
Received 25 April 2016
Received in revised form 3 November 2016
Accepted 5 November 2016
Available online 6 November 2016

Keywords:
Zn
Cd
Carbonate
GEOTRACES

ABSTRACT

Zinc and cadmium are important biologically cycled nutrients in the modern ocean. Recent analytical advances and sampling efforts such as GEOTRACES have led to measurements of the global distribution of Zn and Cd and their stable isotope ratios (δ^{66}Zn and δ^{114}Cd), providing an understanding of how biological processes cycle these elements and their isotopes in the modern ocean. This opens the door to better application of δ^{66}Zn and δ^{114}Cd as tracers of biogeochemical processes archived in the geological record. Here we present new measurements of [Cd] and δ^{114}Cd on samples from the Nuccaleena cap dolostone in South Australia, which was deposited during deglaciation of the ca. 635 Ma old Marinoan snowball Earth. Our new data are combined with previously measured δ^{66}Zn data from the same samples. The combined record of δ^{114}Cd and δ^{66}Zn is used to explore various hypotheses about the sources and sinks of Cd and Zn in the post-Marinoan ocean. Key features of this record are that [Zn] and [Cd] remain relatively similar throughout, that δ^{66}Zn and δ^{114}Cd change at the same stratigraphic level and in the same direction, and that δ^{66}Zn changes are about four times larger than δ^{114}Cd changes even though both quantities reflect a similar fractional mass difference. We suggest that both Zn and Cd concentration and isotopic data are consistent with a change in the sink by which Zn and Cd are removed from the oceans. We propose that no isotope fractionation is expressed during removal of Zn and Cd as sulfides, while Zn and Cd removed with biological material are about 0.6‰ and 0.2‰ lighter than deep ocean δ^{66}Zn and δ^{114}Cd, respectively. Many previous studies attribute the burial of isotopically light biological Zn to preferential assimilation of isotopically lighter Zn by phytoplankton. In contrast, we propose that lighter biological δ^{66}Zn occurs mostly because isotopically heavy Zn was scavenged by organic matter, which causes dissolved δ^{66}Zn in the surface ocean to be lighter than deep ocean δ^{66}Zn. The organic matter originated from primary producers that thrived in the surface ocean during deglaciation. For Cd, whose isotope cycling in the modern ocean is dominated by preferential assimilation of isotopically lighter Cd by phytoplankton, much less biological fractionation is expressed. The combined analyses of δ^{66}Zn and δ^{114}Cd provide insight into the biogeochemical processes which occurred after the Marinoan snowball Earth glaciation, and may be a useful new tool to explore the history of life on Earth in other geological records as well.

1. Introduction

In the modern ocean, the trace-metals zinc (Zn) and cadmium (Cd) have a 'nutrient-type' distribution, with low concentrations in the surface ocean where they are removed from seawater by growing phytoplankton, and higher concentrations in the deep ocean where they are released as sinking organic matter is remineralized. Over the past several years it has become possible to measure the stable isotopes of Zn and Cd in seawater (δ^{66}Zn and δ^{114}Cd, respectively) yielding an understanding of how biological cycling affects these stable isotope ratios in the modern ocean.

This new knowledge increased interest in the application of δ^{66}Zn and δ^{114}Cd as tracers of biological processes in the geological record. For example, δ^{66}Zn in carbonates deposited over the past 175 ky have been related to climatic changes (Pichat et al., 2003), δ^{66}Zn in banded iron formations over the past 3.8 Gy have been related to continental weathering (Pons et al., 2013), and δ^{66}Zn in post-snowball Earth cap dolostones have been related to weathering and biological cycling (Kunzmann et al., 2013). Methods for the analysis of δ^{66}Zn in marine sponges and in diatom frustules have been developed with the aim of utilizing them as archives of past-ocean δ^{66}Zn (Andersen et al., 2011; Hendry and Andersen, 2013). δ^{114}Cd in shales from the Late Permian

* Corresponding author.
E-mail address: sethjohn@usc.edu (S.G. John).

http://dx.doi.org/10.1016/j.palaeo.2016.11.003
0031-0182/

has been used in conjunction with Cd concentrations and $\delta^{15}N$ to infer productivity in the ancient ocean (Georgiev et al., 2015), and methods for the analysis of $\delta^{114}Cd$ in ferromangenese crusts and marine calcites have been developed with the aim of using them as archives of past-ocean $\delta^{114}Cd$ (Horner et al., 2010; Horner et al., 2011).

Although $\delta^{66}Zn$ and $\delta^{114}Cd$ have not previously been used together in the geological record, they present an intriguing pair for geological applications. Zn and Cd are both Group 12 elements in the periodic table (Zn appears just above Cd) meaning that they have the same number of electrons in their outer valence shell, and thus their chemistry is broadly similar. Both elements have a nutrient-like distribution in the modern ocean with similar biological cycling (Fig. 1). However, there are also key differences in the isotopic fractionation of $\delta^{66}Zn$ and $\delta^{114}Cd$ in the ocean, notably the decrease in $\delta^{66}Zn$ towards the surface ocean where $\delta^{114}Cd$ increases (Fig. 1).

Glacial deposits of the ca. 635 Ma old Marinoan glaciation were deposited at low paleolatitudes (e.g., Evans, 2000; Hoffman and Li, 2009; Li et al., 2013) and are sharply but conformably overlain by post-glacial cap carbonate sequences (Hoffman and Schrag, 2002). The basal transgressive systems tract of these sequences is generally referred to as 'cap dolostones', which were deposited during the rise of global mean sea-level resulting from ice-sheet meltdown (Kennedy, 1996; Hoffman et al., 2007). Cap dolostones occur on every paleocontinent, even in siliciclastic-dominated sedimentary successions. They are typically laterally persistent at basinal scale, although their thickness is often strongly controlled by paleotopography (e.g. Hoffman et al., 2011). Deposition during retreat of ice sheets likely lead to cap dolostone precipitation from a low-salinity meltwater plume (Shields, 2005). Furthermore, meltwater injection and surface warming would have caused strong density stratification, possibly leading to physical separation of the surface and deep ocean during deposition of the entire cap dolostone (Shields, 2005). No consensus exists about the duration of cap dolostone formation. While ice sheet melting models and sedimentological considerations indicate deposition in less than 10,000 years (Hyde et al., 2000; Hoffman et al., 2007), paleomagnetic reversals may suggest deposition 1–2 orders of magnitude longer (Trindade et al., 2003; Kilner et al., 2005).

Cap dolostones have attracted significant scientific interest because they record extreme environmental conditions during deglaciation, manifested in unusual sedimentological structures such as sheet-crack cements (Kennedy, 1996; Corkeron, 2007; Hoffman and Macdonald, 2010), tubestone stromatolites (e.g., Cloud et al., 1974; Corsetti and Grotzinger, 2005; Hoffman, 2011), and giant wave ripples (Allen and Hoffman, 2005). Unique paleoenvironmental conditions during cap dolostone deposition are also inferred from geochemical records, including non-traditional stable isotopes. Boron isotopes have been interpreted to reflect initial ocean acidification during deglaciation (Kasemann et al., 2005, 2010; Ohnemüller et al., 2014), Ca and Mg isotopes suggest high continental weathering rates, dominated by carbonate supply during cap dolostone deposition (Silva-Tamayo et al., 2010; Kasemann et al., 2014), and triple oxygen isotopes indicate elevated atmospheric CO_2 levels in the aftermath of the Marinoan glaciation (Bao et al., 2008).

The Nuccaleena cap dolostone is an ideal target to test the paired application of $\delta^{114}Cd$ along with the existing $\delta^{66}Zn$ record for four reasons: 1) prior work has suggested that the $\delta^{66}Zn$ record is free from diagenetic alteration and free from significant amounts of contaminating phases such as oxide coatings (Kunzmann et al., 2013); 2) $\delta^{66}Zn$ changes in clear trends which seem to record large changes in the geological environment (Kunzmann et al., 2013) and cap dolostones typically record large signals and significant variation in geochemical proxies reflecting extreme environmental conditions during deposition; 3) coupled Zn and Cd isotopes have the potential to shed light on a geologically interesting but poorly understood time in Earth's history and 4) previous interpretations of the $\delta^{66}Zn$ record seem to be inconsistent with more recent evidence about the distribution of $\delta^{66}Zn$ and $\delta^{114}Cd$ in seawater. We have therefore measured $\delta^{114}Cd$ on the same samples which were analyzed for $\delta^{66}Zn$ by Kunzmann et al. (2013), both in order to gain a better understanding of what these records can tell us about the Earth during deglaciation from the Marinoan snowball Earth, and as an opportunity to explore how paired analyses of $\delta^{66}Zn$ and $\delta^{114}Cd$ might be applied elsewhere in the geological record. Building on a previous study of [Zn] and $\delta^{66}Zn$ in post-snowball Earth cap dolostones (Kunzmann et al., 2013), we present new data on [Cd] and $\delta^{114}Cd$ on the same samples, and apply our principles to better understand how Earth's history is recorded in $\delta^{66}Zn$ and $\delta^{114}Cd$.

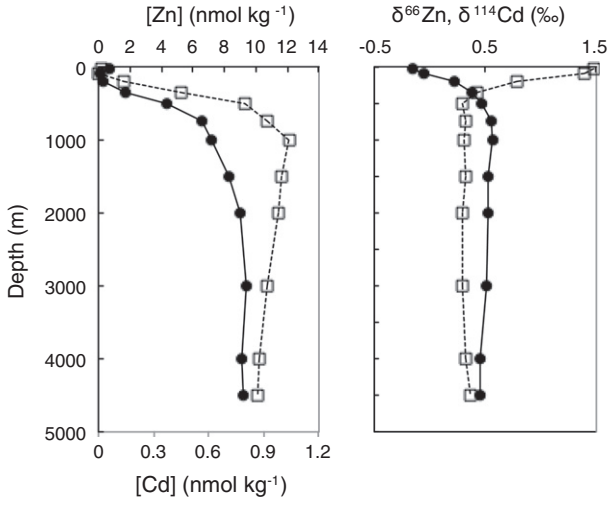

Fig. 1. Zn and Cd concentrations and stable isotope ratios from the North Pacific (SAFe site, Conway and John, 2015b) are typical of global distributions. Both [Zn] (black circles) and [Cd] (white squares) decrease towards the surface ocean due to biological uptake. $\delta^{114}Cd$ increases towards the surface ocean whereas $\delta^{66}Zn$ decreases.

2. Sample material and methods

2.1. Sampled section

The samples investigated in this study come from a section of the Nuccaleena cap dolostone (previously reported in Kunzmann et al., 2013) that conformably overlies glacial deposits of the Elatina Formation in the Adelaide Rift Complex of South Australia (Fig. S1). The lowermost ~8.5 m of the section consists of buff-yellow, fine grained dolostone, overlain by ca. 1 m of interbedded dolostone and purple shale. Above ca. 9.5 m, purple shale beds dominate and dolostone beds gradually disappear upsection. The contact to the following Brachina Formation is gradational and occurs with the last dolostone bed at ca. 14 m.

2.2. Methods

$\delta^{66}Zn$, [Cd], and $\delta^{114}Cd$ measurements were carried out on new powders of the samples studied by Kunzmann et al. (2013). Sample cleaning, purification, and analysis was undertaken at the University of South Carolina according to the same procedures used by Kunzmann et al. (2013). Samples were cleaned by sonication three times with ethanol then ultrapure water, and dissolved in 1.5 M acetic acid. This method is designed to selectively leach carbonate, without dissolving significant amounts of contaminating phases such as oxide coatings, clays, or other lithogenic materials (Pichat et al., 2003; Kunzmann et al., 2013). Lack of correlation between $\delta^{66}Zn$ and P, Al, Fe, and Mn concentrations in the studied samples demonstrate the reliability of this selective leaching technique (Kunzmann et al., 2013). The concentration of Cd in the carbonates was determined on an Element single-collector ICPMS using In to monitor instrumental sensitivity

compared to a multi-element standard. Samples were amended with ^{64}Zn–^{67}Zn and ^{110}Cd–^{111}Cd double spikes in a 1:2 and 1:4 sample:spike ratio, respectively, to minimize analytical error (John, 2012). Then, samples were purified by anion exchange chromatography based on methods developed for analysis of $\delta^{66}Zn$ and $\delta^{114}Cd$ in seawater (Conway et al., 2013), but modified with 6.75 times greater eluent volumes and larger columns with 135 μL of AG-MP1 resin (Revels et al., 2014). After purification, samples were analyzed for $\delta^{66}Zn$ and $\delta^{114}Cd$ on a Neptune multi-collector ICPMS at the University of South Carolina.

Initial measurements of carbonate $\delta^{114}Cd$ contained four outlier data points suggesting poor data quality. Most samples followed a gradual trend similar to $\delta^{66}Zn$ but these four samples were ~1–2‰ lighter than nearby samples. The $\delta^{114}Cd$ of these outlier samples was also very sensitive to the Pd correction applied by monitoring mass 105 for ^{105}Pd and correcting for the presence of ^{110}Pd at mass 110, suggesting either high amounts of Pd in the samples or some other interference at mass 105. $\delta^{114}Cd$ samples were therefore purified a second time through the same anion exchange chromatography and reanalyzed to produce the data presented here. After this second purification there was very little signal at mass 105 and no data points lying far outside the overall trend, suggesting high-quality data. The $\delta^{114}Cd$ of samples which were not obvious outliers after the first purification did not change significantly after the second purification, suggesting that they had not been affected by an interference.

3. Results

Zinc stable isotope ratios ($\delta^{66}Zn$) measured here are very similar to values presented in Kunzmann et al. (2013) (Fig. S1). The external error for duplicates run between different laboratories is roughly 40% higher than would be predicted by the internal errors reported by each lab, suggesting slight $\delta^{66}Zn$ inhomogeneity between different powders from the same samples. Still, the difference between $\delta^{66}Zn$ measured by each lab is generally less than 0.1‰, and both datasets clearly show the same overall trends in $\delta^{66}Zn$, indicating excellent overall reproducibility even on samples which were separately crushed, cleaned, purified, and analyzed in different laboratories (Fig. S2).

[Cd] in the carbonate samples shows patterns very similar to the [Zn] values measured by Kunzmann et al. (2013). Both [Zn] and [Cd] decrease slightly over the first 10 m of the section and then increase sharply to higher values around 12 m to 14 m (Fig. 2). The Zn/Cd ratio is similar to the crustal abundance ratio of these elements (Fig. 3). Estimates of the relative crustal abundances of Zn and Cd vary considerably, but the Zn/Cd ratios in our samples fall well within the ranges reported for eleven different studies which estimated crustal abundances of Zn and Cd as summarized by Hu and Gao (2008) (Fig. 4).

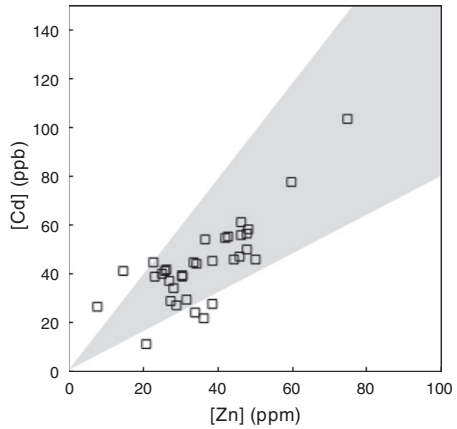

Fig. 3. Correspondence between [Zn] and [Cd] measured in carbonate samples. The grey shaded area represents a range of estimates of the crustal Zn/Cd ratio as summarized by Hu and Gao (2008).

$\delta^{114}Cd$ changes over the section in a fashion similar to changes in $\delta^{66}Zn$, though with larger analytical errors and scatter among data (Fig. 2). Both datasets show an overall trend of decreasing $\delta^{66}Zn$ or $\delta^{114}Cd$ over the first ~10 m of the section, and a dramatic increase between 10 m and 14 m. The increase in $\delta^{66}Zn$ from the lowest values at 6–8 m to the highest values at 10–14 m is approximately 0.8‰, while the change in $\delta^{114}Cd$ over the same interval is approximately 0.2‰.

4. Discussion

Our new data on $\delta^{114}Cd$ allows us to reconsider the history of post-Marinoan marine environments recorded in the Nuccaleena cap dolostone. Similar to Kunzmann et al. (2013), we assume that the marine cycling of Zn and Cd were dominated by one process during the early and late intervals of carbonate deposition (0–3 m and 10–14 m, when both $\delta^{66}Zn$ and $\delta^{114}Cd$ are higher) and were dominated by a different process during the middle interval (3–10 m, when $\delta^{66}Zn$ and $\delta^{114}Cd$ are lower). We consider a variety of different processes which might control $\delta^{66}Zn$ and $\delta^{114}Cd$ including biological productivity in the surface ocean, increased flux of continental Zn and Cd to the ocean, sulfide precipitation, and biological assimilation of Zn and Cd. In evaluating each of these processes we consider three key features of the Nuccaleena cap dolostone Zn and Cd records:

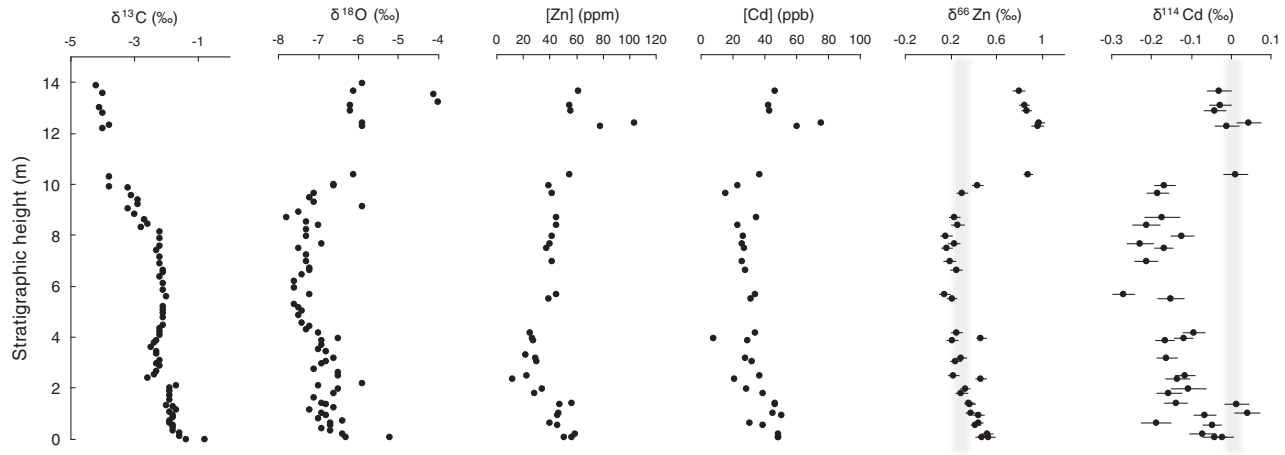

Fig. 2. Analyses of parameters for carbonate samples from the Nuccaleena cap dolostone. $\delta^{13}C$, $\delta^{18}O$, and [Zn] are taken from Kunzmann et al. (2013) while other data are from this study. Grey bars represent the $\delta^{66}Zn$ and $\delta^{114}Cd$ range for inputs to the ocean.

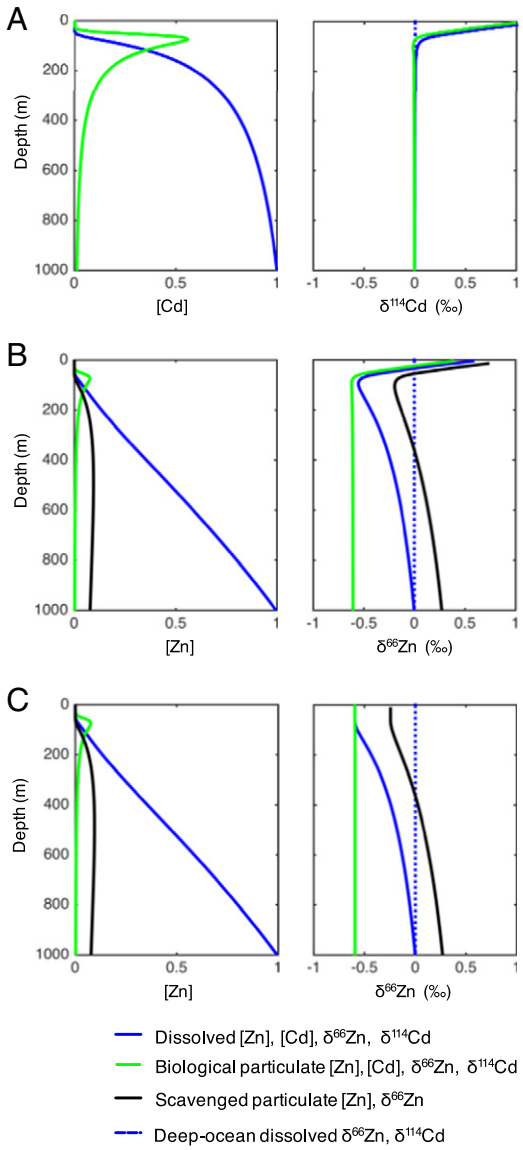

Fig. 4. Model concentrations and stable isotope ratios representing the cycling of Cd and Zn in the upper ocean. For Cd, biological assimilation is the only process removing dissolved Cd. An assumed biological assimilation isotope effect of −0.2‰ leads to an increase in dissolved and biological particulate δ^{114}Cd in the surface ocean, but below ~100 m the total δ^{114}Cd for sinking biological particulates is equal to the deep ocean dissolved δ^{114}Cd ($\Delta^{114}Cd_{biological} = 0‰$) (A). Zn is removed from the dissolved phase both by biological assimilation and by scavenging onto sinking biological particles as in John and Conway (2013). A model run with a −0.2‰ isotope effect for biological assimilation leads to an increase in dissolved, biological, and scavenged δ^{66}Zn above 100 m (B). With a biological assimilation isotope effect of 0‰, δ^{66}Zn does not increase near the surface (C). In both Zn models, scavenging causes dissolved δ^{66}Zn to decrease towards the surface ocean, so that the biological particulate δ^{66}Zn produced in the surface ocean which subsequently sinks to 1000 m is lower than deep ocean dissolved δ^{66}Zn ($\Delta^{66}Zn_{biological} = -0.6‰$). This model assumes deep ocean δ^{66}Zn and δ^{114}Cd of 0‰, though of course the patterns would be the same for a different values.

1) [Zn] and [Cd] covary within the record, being lower in the middle interval compared to top and bottom of the section.
2) δ^{66}Zn and δ^{114}Cd covary within the record, being lower in the middle interval compared to top and bottom of the section.
3) The magnitude of variation in δ^{66}Zn is about four times greater than for δ^{114}Cd, despite similar fractional mass differences in ^{66}Zn/^{64}Zn and ^{114}Cd/^{110}Cd.

We assume that carbonate δ^{66}Zn reflects seawater δ^{66}Zn without any isotope fractionation, based on both field observations which show no difference between modern marine carbonate δ^{66}Zn and seawater (Pichat et al., 2003) and laboratory experiments which show little fractionation as Zn interacts with carbonates (Maréchal and Sheppard, 2002; Dong and Wasylenki, 2013). In contrast, laboratory experiments do show Cd isotope fractionation during carbonate precipitation (Horner et al., 2011). Carbonate δ^{114}Cd was found to be −0.45‰ lighter than seawater at modern ocean salinities decreasing to 0‰ in freshwater. Considering the low salinities of surface waters in the post-snowball earth ocean (Shields, 2005), some of the variability in carbonate δ^{114}Cd may result from changes in salinity and carbonate δ^{114}Cd may have been slightly offset from seawater δ^{114}Cd when samples were deposited, as discussed below.

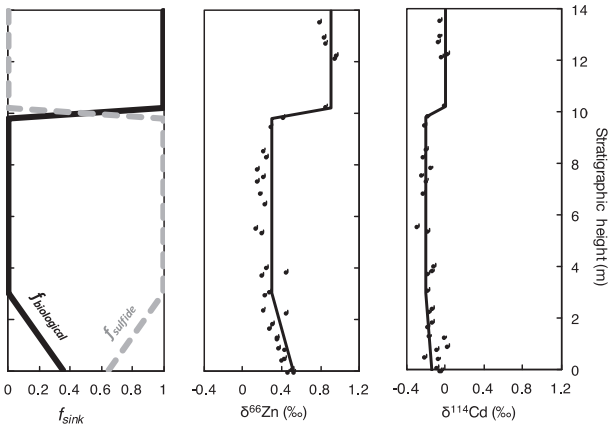

Fig. 5. The observed trends in δ^{66}Zn and δ^{114}Cd can be reproduced with a simple model which assumes a change in the sinks for Zn and Cd from the oceans, each of which has a different value of Δ.

4.1. Surface ocean biological productivity

Kunzmann et al. (2013) interpret the higher δ^{66}Zn observed in the early and late intervals as reflecting an increase in surface ocean δ^{66}Zn due to the removal of isotopically light Zn by biological processes. This interpretation is consistent with the observed biological preference for assimilation of isotopically light Zn in culture (John et al., 2007; John and Conway, 2013). However, it is at odds with observations of either invariant or decreasing δ^{66}Zn towards the surface in the modern ocean (Zhao et al., 2013; Conway and John, 2014; Conway and John, 2015b). Furthermore, modern ocean δ^{66}Zn and δ^{114}Cd vary in different directions towards the surface ocean, with δ^{66}Zn decreasing and δ^{114}Cd increasing (Fig. 1). Thus, it is unlikely that the Nuccaleena cap dolostone records the biological drawdown of Zn and Cd in the surface ocean.

4.2. Increased weathering flux of Zn and Cd

Kunzmann et al. (2013) observed that carbonate δ^{66}Zn during the middle interval was similar to the δ^{66}Zn of lithogenic inputs (Fig. 2), and therefore interpreted the lower δ^{66}Zn in the middle interval as reflecting an increased weathering supply of Zn to the oceans, caused by the postulated post-glacial supergreenhouse climate (Hoffman and Schrag, 2002). At steady state, the isotope composition of the oceans can be expressed as:

$$\delta_{ocean} = \delta_{sources} - \Delta_{sinks} \quad (1)$$

where δ_{ocean} is the mean ocean δ^{66}Zn or δ^{114}Cd, $\delta_{sources}$ is the isotopic composition of the sources, and Δ_{sinks} is the isotopic offset between ocean δ^{66}Zn or δ^{114}Cd and sink δ^{66}Zn or δ^{114}Cd (e.g. $\delta^{66}Zn_{sinks} - \delta^{66}Zn_{ocean}$). Thus, if the increased weathering flux of Zn and Cd to the oceans was balanced by a similar increase in their sinks (i.e., steady state), and the character of the sink did not change, marine δ^{66}Zn and

δ^{114}Cd would not change. In order for increased weathering flux alone to drive marine δ^{66}Zn and δ^{114}Cd towards continental values, the large increase in Zn and Cd inputs to the oceans would have to occur without a similar increase in sink magnitude. However, this would lead to a dramatic increase in marine concentrations of Zn and Cd, while observations point to lower concentrations of these elements as reflected in decreasing Zn/Ca and Cd/Ca ratios during the middle interval compared to early and late intervals.

4.3. Changes in the marine sink for Zn and Cd

Having discounted the above processes as the cause of the δ^{66}Zn and δ^{114}Cd decline in the middle part of the section, we are left to consider whether the whole surface ocean δ^{66}Zn and δ^{114}Cd might have varied due to a change in the sink by which Zn and Cd leave the ocean. The important sources of Zn to the ocean have previously been determined to have δ^{66}Zn values similar to crustal values (Little et al., 2014; Little et al., 2016). Here we have compiled data about Cd inputs to the ocean and find that they are also within error of crustal values (Table 1). If we assume that carbonate δ^{66}Zn reflects seawater values, then the crustal δ^{66}Zn values during the middle interval indicate $\Delta_{sinks} \approx 0$, while the values during the early and late interval suggest $\Delta_{sinks} \approx -0.4$ to -0.8‰. δ^{114}Cd values slightly decline in the middle part of the section suggesting $\Delta_{sinks} \approx 0.2$‰. This minor shift may record primary changes in seawater δ^{114}Cd, which does not seem unlikely as it parallels δ^{66}Zn. Alternatively, this could be explained by an isotope effect during the incorporation of Cd into carbonate, measured at 0 to -0.45‰ for calcite (Horner et al., 2011), requiring a systematic change in oceanographic conditions or mineralogical composition during deposition of the middle part of the cap dolostone. The modern ocean is isotopically heavy with respect to inputs for both Zn and Cd, just as we infer for the early and late intervals, suggesting a sink for isotopically light Zn and Cd. The nature of this sink in the modern ocean is not known for either Zn or Cd, though in both cases the precipitation of isotopically light sulfides has been hypothesized as a possible cause (Janssen et al., 2014; Conway and John, 2015a). There is experimental evidence for precipitation of isotopically light ZnS (Archer et al., 2004), observational evidence for the precipitation of isotopically light CdS (Janssen et al., 2014), and theoretical studies show that dissolved sulfide species of both elements are isotopically lighter than chloride and hydroxide species at equilibrium (Fujii et al., 2011; Yang et al., 2015). However, a recent study which differentiates between organic Zn and sulfide Zn in sulfidic sediments shows that Zn sulfides are isotopically similar to deep-ocean Zn (Tang et al., 2016). In addition, other isotope systems also suggests sulfide precipitation in the modern ocean are not sinks for isotopically light Zn and Cd. Zn and Cd are both chalcophile elements which readily precipitate in the presence of sulfide, meaning that they are likely to be quantitatively lost at sulfide gradients, similar to the closed-system isotope systematics of Mo sulfide precipitation and sedimentary denitrification. In both cases closed-system isotope systematics dominate and either none or very little of the instantaneous isotope effect is expressed (e.g. Arnold et al., 2004; Lehmann et al., 2007). Finally, the lack of large changes in δ^{114}Cd suggests that sulfide precipitation is not the cause of heavy δ^{66}Zn values in the Nuccaleena cap dolostone. Even in a case where sulfide is slowly titrated into the ocean, such that ZnS precipitates under open-system conditions and an isotope effect can be expressed, CdS would also be expected to precipitate. Theoretical predictions suggest a similar $\Delta_{sulfide}$ for Cd and Zn (Fujii et al., 2011; Yang et al., 2015), and CdS has a lower solubility constant than ZnS, so there is no clear mechanism by which ZnS could precipitate under open system conditions while CdS does not. Thus the much larger changes in δ^{66}Zn compared to δ^{114}Cd provide additional evidence that sulfide precipitation was not the cause of higher δ^{66}Zn during the early and late intervals.

Instead, we propose that heavy marine δ^{66}Zn in the early and late intervals is due to the burial of isotopically light organic Zn. The biological productivity hypothesis discussed in Section 4.1 considers just the net effect of biological productivity, which is shown to remove isotopically heavier Zn from the modern surface ocean. In contrast, our explanation relies on phytoplankton containing both an isotopically lighter assimilated Zn phase and an isotopically heavier adsorbed Zn phase (Fig. 4). The adsorption of isotopically heavy Zn has previously been observed onto phytoplankton grown in culture (Gélabert et al., 2006; John and Conway, 2013; Coutaud et al., 2014), leading to the suggestion that the decrease in δ^{66}Zn towards the modern surface ocean may be driven by scavenging of isotopically heavy Zn onto sinking biogenic particles (John and Conway, 2013). Cd isotope cycling in the modern ocean is thought to be controlled by biological assimilation alone, with no contribution from scavenging. When Cd is quantitatively assimilated in the surface ocean, as it is in much of the modern ocean, the δ^{114}Cd of particulate material exported from the surface ocean is the same as deep-ocean δ^{114}Cd ($\Delta_{biological} = 0$‰, Fig. 4). This would explain why δ^{114}Cd does not change very much in our sampled section, while δ^{66}Zn changes significantly. To the extent that δ^{114}Cd does increase slightly in the lower and upper intervals, it could be due to non-quantitative uptake of Cd in some parts of the ocean, similar to how Cd uptake in the modern Southern Ocean is not quantitative and therefore phytoplankton which grow in the surface ocean and remineralize in the deep ocean may have a Cd isotope composition which is lighter than deep ocean δ^{114}Cd. Alternatively, this signal might be due to changes in the isotope effect of Cd incorporation into carbonate caused by changes in ocean salinity during deglaciation, when the surface ocean generally had a low salinity due to melting sea ice (Shields, 2005), which may have been stratigraphically and spatially heterogeneous.

During the middle interval, Δ_{sinks} for both Zn and Cd would have been close to 0‰, consistent with a switch in the sink from primarily biological material to primarily sulfides. Based on analyses from the Cariaco Basin, Tang et al. find that sulfide δ^{66}Zn matches deep-ocean δ^{66}Zn (Tang et al., 2016). As discussed above, this likely results from closed-system behavior where all of the Zn is precipitated in the presence of sulfide, even though there may be an instantaneous isotope effect for sulfide precipitation. Because Cd precipitates even more readily than Zn in the presence of sulfide, we presume that the sink for Cd would also have switched from burial of organic material to burial of sulfides. However, since both sinks have an Δ_{sinks} close to 0, this results in little change in marine δ^{114}Cd recorded in carbonate.

Table 1
Mean δ^{66}Zn and δ^{114}Cd for some of the most important reservoirs, sources, and sinks of Zn and Cd in the modern ocean. Full data are presented in Supplementary Table S1. Data is taken from 1) Little et al., 2016, and references therein, 2) Little et al., 2014, and references therein, 3) Tang et al., 2016, 4) Schmitt et al., 2009, 5) Ripperger et al., 2007; Xue et al., 2013; Conway and John, 2015a; Conway and John, 2015b, 6) Lambelet et al., 2013, 7) Schmitt et al., 2009; Abouchami et al., 2015, 8) Schmitt et al., 2009; Horner et al., 2010.

	δ^{66}Zn (‰)	1σ SD	*n*	Refs.	δ^{114}Cd (‰)	1σ SD	*n*	Refs.
Reservoirs								
Lithosphere	0.27	0.07	50	1	−0.04	0.05	4	4
Ocean	0.49	0.07	116	1	0.38	0.07	299	5
Sources								
Rivers	0.33		32	1	0.24	0.27	8	6
Aeolian dust	0.32	0.14	30	1	−0.02	0.04	3	4
Hydrothermal	0.24	–	–	2	0.06	0.06	4	7
Sinks								
Fe-Mn sediments	0.96	0.15	69	1	0.23	0.11	54	8
Biogenic carbonate	1.07	0.14	26	1	–	–	–	
Opal	0.03	0.19	20	1	–	–	–	
Sedimentary sulfides	~0.5	–	–	3	–	–	–	
Sedimentary organics	−0.1	–	–	–	–	–	–	

4.4. Model $\delta^{66}Zn$ and $\delta^{114}Cd$

Our hypothesis that the Nuccaleena cap dolostone $\delta^{66}Zn$ and $\delta^{114}Cd$ records reflect a switch in sinks for these elements from the ocean can be expressed in a quantitative model, allowing us to constrain some relevant isotope effects (Fig. 5). Expanding the steady-state mass balance for the oceans from Eq. (1), the measured carbonate Zn isotope ratio ($\delta^{66}Zn_{carbonate}$) can be described by:

$$\delta^{66}Zn_{carbonate} = \delta^{66}Zn_{sources} - f_{biological}\cdot\Delta^{66}Zn_{biological} - f_{sulfide}\cdot\Delta^{66}Zn_{sulfide} - \Delta^{66}Zn_{carbonate} \quad (2)$$

where $f_{biological}$ is the fraction of Zn buried as assimilated biological Zn and it has an isotope composition offset from ocean $\delta^{66}Zn$ by a value of $\Delta^{66}Zn_{biological}$, $f_{sulfide}$ is similarly the fraction of Zn buried as sulfide with an isotopic offset from mean ocean $\delta^{66}Zn$ of $\Delta^{66}Zn_{sulfide}$, and $\Delta^{66}Zn_{carbonate}$ is the offset between ocean $\delta^{66}Zn$ and carbonate $\delta^{66}Zn$. An equivalent expression can be written for $\delta^{114}Cd$.

For Zn, we assume that sources have a $\delta^{66}Zn$ of +0.3‰ (Little et al., 2014) and that $\Delta^{66}Zn_{carbonate}$ is 0‰ (Maréchal and Sheppard, 2002; Pichat et al., 2003; Kunzmann et al., 2013; Dong and Wasylenki, 2013). We assume that the dominant sink for Zn during the middle interval is sulfides ($f_{sulfide} = 1$) and during the late interval is biological ($f_{biological} = 1$). In order to match the observed increase in $\delta^{66}Zn_{carbonate}$ during the upper interval, we set $\Delta^{66}Zn_{biological}$ to −0.6‰. Much of this offset can be attributed to the fact that surface seawater is about 0.5‰ lighter than deep seawater in much of the modern surface ocean (Conway and John, 2014; Conway and John, 2015b), and is thus independent of the isotope effect for biological assimilation (Fig. 4). Additionally, cultured phytoplankton growing at typical modern ocean Zn concentrations preferentially assimilate lighter Zn with an isotope effect of −0.2‰ (John et al., 2007), suggesting that biological material could be up to −0.7‰ lighter than seawater if surface Zn uptake is not quantitative. The gradual decrease in $\delta^{66}Zn_{carbonate}$ in the lower interval is accounted for by a linear decrease in $f_{biological}$ from 0.35 to 0.

The same switch between biological and sulfide sinks can account for the carbonate $\delta^{114}Cd$ record. Sources of Cd to the oceans are all within error of 0‰. However, $\delta^{114}Cd_{carbonate}$ is −0.2‰ during the middle interval when we assume that $f_{sulfide}$ is 1 and $\Delta^{114}Cd_{sulfide} = 0$, suggesting an isotope effect during Cd incorporation into carbonate of $\Delta^{114}Cd_{carbonate} = -0.2$‰. This is within the overall range of observed isotope effects during calcite precipitation between 0‰ in fresh water and −0.45‰ at modern ocean salinity (Horner et al., 2011). Therefore, an isotopic offset of about −0.2‰ is consistent with the assumption of a low-salinity surface ocean during deglaciation (Shields, 2005) but isotopic fractionation during Cd incorporation may have also been affected by a more Mg-rich primary carbonate mineralogy than pure calcite. During the lower and upper intervals $\delta^{114}Cd_{carbonate}$ is slightly heavier, suggesting a $\Delta^{114}Cd_{biological}$ of around −0.2‰. The instantaneous isotope effect for phytoplankton in the Southern ocean is between −0.2‰ to −0.4‰, depending on the region (Abouchami et al., 2011), meaning that the modeled $\Delta^{114}Cd_{biological} = -0.2$‰ could result from non-quantitative uptake of Cd in the surface oceans.

It is unclear whether the postulated sulfide sink during deposition of the middle portion of the Nuccaleena cap dolostone requires basin/shelf scale euxinia (anoxic and free hydrogen sulfide) or if significant dissolved pore water sulfide concentrations are sufficient to quantitatively remove Zn and Cd from seawater. Oceanic redox conditions post-dating cap dolostones have been studied in several basins and paleoredox data from shales immediately overlying the Doushantuo cap dolostone in South China indicate deposition under euxinic conditions (Sahoo et al., 2012), whereas data from coeval shales in NW Canada and Svalbard demonstrate the dominance of ferruginous (anoxic and dissolved Fe(II)) conditions on continental shelves (Johnston et al., 2013; Kunzmann et al., 2015). However, paleoredox conditions and potential water column stratification during cap dolostone deposition are poorly understood. The ocean may have been characterized by an oxic surface layer, an anoxic intermediate layer (due to organic matter oxidation), and an anoxic deep layer characterized by geochemically–evolved snowball Earth brine (Hoffman, pers. com.). Depending on nutrient fluxes, the intermediate layer may locally have been euxinic, representing a water column sulfide sink for Zn and Cd.

In summary, we suggest that $\delta^{66}Zn$ and $\delta^{114}Cd$ signals recorded in the Nuccaleena cap dolostone record the varying significance of biological and sulfide sinks in the post-Marinoan ocean. When sulfide minerals are negligible, the primary sink for Zn and Cd is organic matter. Our interpretation that geological variability in $\delta^{66}Zn$ reflects changes in biological versus sulfide sinks for Zn is quite different from other studies which apply $\delta^{66}Zn$ as a geological proxy (Maréchal et al., 2000; Pichat et al., 2003; Andersen et al., 2011; Hendry and Andersen, 2013; Kunzmann et al., 2013). Considering the most recent results from studies on modern ocean Zn cycling, we significantly revise the original Zn isotope interpretation by Kunzmann et al. (2013). Although our new results confirm evidence for immediate resumption of primary productivity after snowball Earth, we propose that elevated $\delta^{66}Zn$ values in the lower and upper parts of the Nuccaleena cap dolostone can be explained by incorporation of isotopically light Zn into organic matter, driving the surface ocean isotopically heavier. The decline in $\delta^{66}Zn$ in the middle portion of the cap dolostone can be explained by significant incorporation of Zn in sulfide minerals.

5. Conclusions

This work illustrates the potential value of pairing $\delta^{66}Zn$ and $\delta^{114}Cd$ analyses in the geological record. Zn and Cd have similar sources to the ocean and similar internal cycling as micronutrients. However, there are also dramatic differences in their isotopic cycling, particularly their opposite fractionation during biological cycling in the upper ocean. These similarities and differences make it possible to interpret paired records of $\delta^{66}Zn$ and $\delta^{114}Cd$ with more confidence than either record alone. In addition to proposing a new framework for interpreting carbonate $\delta^{66}Zn$ and $\delta^{114}Cd$ following the Marinoan glaciation, we hope that this study can provide insight into the ways in which $\delta^{66}Zn$ and $\delta^{114}Cd$ might be used as geological proxies in other contexts. The future utility of paired $\delta^{66}Zn$ and $\delta^{114}Cd$ analyses can be further enhanced by experiments in which both isotopic systems are measured in tandem. Further work on understanding the global extent of changes in $\delta^{66}Zn$ and $\delta^{114}Cd$ following glaciations and mass extinction events, and further experimental work to constrain important isotopic fractionation factors, will help to distinguish between various possible interpretations of the geological record. As our understanding of $\delta^{66}Zn$ and $\delta^{114}Cd$ grows, it will be possible to better use these tracers to support or reject hypotheses about Zn and Cd, and their interactions with biological and geological processes recorded in the rock record.

Acknowledgments

We thank Tim Raub and Isaac Hilburn for help in the field, and Frank Corsetti and Paul Hoffman for helpful discussions during the writing of this manuscript. We thank Susan Little and an anonymous reviewer for comments on this manuscript. MK publishes with permission of the Executive Director of the Northern Territory Geological Survey. This study was funded by the National Science Foundation (OCE-1235150).

Appendix A. Supplementary data

Supplementary data to this article can be found online at http://dx.doi.org/10.1016/j.palaeo.2016.11.003.

References

Abouchami, W., Galer, S.J.G., de Baar, H.J.W., Alderkamp, A.C., Middag, R., Laan, P., Feldmann, H., Andreae, M.O., 2011. Modulation of the Southern Ocean cadmium isotope signature by ocean circulation and primary productivity. Earth Planet. Sci. Lett. 305, 83–91.

Abouchami, W., Koschinsky, A., Haßler, K., Galer, S.J.G., 2015. Cadmium and lead isotopes in high temperature hydrothermal vents on the Mid-Atlantic Ridge. in: Goldschmidt Abstracts 8.

Allen, P.A., Hoffman, P.F., 2005. Extreme winds and waves in the aftermath of a Neoproterozoic glaciation. Nature 433, 123–127.

Andersen, M.B., Vance, D., Archer, C., Anderson, R.F., Ellwood, M.J., Allen, C.S., 2011. The Zn abundance and isotopic composition of diatom frustules, a proxy for Zn availability in ocean surface seawater. Earth Planet. Sci. Lett. 301, 137–145.

Archer, C., Vance, D., Butler, I., 2004. Abiotic Zn isotope fractionations associated with ZnS precipitation. Geochim. Cosmochim. Acta 68, A325.

Arnold, G.L., Anbar, A.D., Barling, J., Lyons, T.W., 2004. Molybdenum isotope evidence for widespread anoxia in mid–Proterozoic oceans. Science 304, 87–90.

Bao, H., Lyons, J.R., Zhou, C., 2008. Triple oxygen isotope evidence for elevated CO_2 levels after a Neoproterozoic glaciation. Nature 452, 504–506.

Cloud, P., Wright, L.A., Williams, E.G., Diehl, P., Walter, M.R., 1974. Giant stromatolites and associated vertical tubes from the upper Proterozoic Noonday Dolomite, Death Valley Region, eastern California. Geol. Soc. Am. Bull. 85, 1869–1882.

Conway, T.M., John, S.G., 2015a. Biogeochemical cycling of cadmium isotopes along a high–resolution section through the North Atlantic Ocean. Geochim. Cosmochim. Acta 148, 269–283.

Conway, T.M., John, S.G., 2014. The biogeochemical cycling of zinc and zinc isotopes in the North Atlantic Ocean. Glob. Biogeochem. Cycles 28, 1111–1128.

Conway, T.M., John, S.G., 2015b. The cycling of iron, zinc and cadmium in the North East Pacific Ocean — insights from stable isotopes. Geochim. Cosmochim. Acta 164, 262–283.

Conway, T.M., Rosenberg, A.D., Adkins, J.F., John, S.G., 2013. A new method for precise determination of iron, zinc and cadmium stable isotope ratios in seawater by double-spike mass spectrometry. Anal. Chim. Acta 793, 44–52.

Corkeron, M., 2007. 'Cap carbonates' and Neoproterozoic glaciogenic successions from the Kimberley region, north-west Australia. Sedimentology 54, 871–903.

Corsetti, F.A., Grotzinger, J.P., 2005. Origin and significance of tube structures in Neoproterozoic post-glacial cap carbonates: example from Noonday Dolomite, Death Valley, United States. PALAIOS 20, 348–363.

Coutaud, A., Meheut, M., Viers, J., Rols, J.-L., Pokrovsky, O.S., 2014. Zn isotope fractionation during interaction with phototrophic biofilm. Chem. Geol. 390, 46–60.

Dong, S., Wasylenki, L., 2013. Zinc isotope fractionation during adsorption on calcite. AGU Conference Abstracts (V51A-2623).

Evans, D.A.D., 2000. Stratigraphic, geochronological, and paleomagnetic constraints upon the Neoproterozoic climatic paradox. Am. J. Sci. 300, 347–433.

Fujii, T., Moynier, F., Pons, M.-L., Albarède, F., 2011. The origin of Zn isotope fractionation in sulfides. Geochim. Cosmochim. Acta 75, 7632–7643.

Gélabert, A., Pokrovsky, O.S., Viers, J., Schott, J., Boudou, A., Feurtet-Mazel, A., 2006. Interaction between zinc and freshwater and marine diatom species: surface complexation and Zn isotope fractionation. Geochim. Cosmochim. Acta 70, 839–857.

Georgiev, S.V., Horner, T.J., Stein, H.J., Bingen, B., Rehkamper, M., 2015. Cadmium-isotopic evidence for increasing primary productivity during the Late Permian anoxic event. Earth Planet. Sci. Lett. 410, 84–96.

Hendry, K.R., Andersen, M.B., 2013. The zinc isotopic composition of siliceous marine sponges: investigating nature's sediment traps. Chem. Geol. 354, 33–41.

Hoffman, P.F., Schrag, D.P., 2002. The snowball Earth hypothesis: testing the limits of global change. Terra Nova 14, 129–155.

Hoffman, P.F., Halverson, G.P., Domack, E.W., Husson, J.M., Higgins, J.A., Schrag, D.P., 2007. Are basal Ediacaran (635 Ma) post-glacial "cap dolostones" diachronous? Earth Planet. Sci. Lett. 258, 114–131.

Hoffman, P.F., Li, Z.-X., 2009. A palaeogeographic context for Neoproterozoic glaciation. Palaeogeogr. Palaeoclimatol. Palaeoecol. 277, 158–172.

Hoffman, P.F., Macdonald, F.A., 2010. Sheet-crack cements and early regression in Marinoan (635 Ma) cap dolostones: regional benchmarks of vanishing ice-sheets? Earth Planet. Sci. Lett. 300, 374–384.

Hoffman, P.F., Macdonald, F.A., Halverson, G.P., 2011. Chemical sediments associated with Neoproterozoic glaciation: iron formation, cap carbonate, barite, and phosphorite. In: Arnoud, E., Halverson, G.P., Schields-Zhou, G. (Eds.), The Geological Record of Neoproterozoic Glaciations. Geological Society, London, Memoirs 36, pp. 67–80.

Hoffman, P.F., 2011. Strange bedfellows: glacial diamictite and cap carbonate from the Marinoan (635 Ma) glaciation in Namibia. Sedimentology 58, 57–119.

Horner, T.J., Rickaby, R.E.M., Henderson, G.M., 2011. Isotopic fractionation of cadmium into calcite. Earth Planet. Sci. Lett. 312, 243–253.

Horner, T.J., Schönbächler, M., Rehkämper, M., Nielsen, S.G., Williams, H., Halliday, A., Xue, Z., Hein, J.R., 2010. Ferromanganese crusts as archives of deep water Cd isotope compositions. Geochem. Geophys. Geosyst. 11, Q04001. http://dx.doi.org/10.1029/2009gc002987.

Hu, Z., Gao, S., 2008. Upper crustal abundances of trace elements: a revision and update. Chem. Geol. 253, 205–221.

Hyde, W.T., Crowley, T.J., Baum, S.K., Peltier, W.R., 2000. Neoproterozoic 'snowball Earth' simulations with a coupled climate/icesheet model. Nature 405, 425–429.

Janssen, D.J., Conway, T.M., John, S.G., Christian, J.R., Kramer, D.I., Pedersen, T.F., Cullen, J.T., 2014. Undocumented water column sink for cadmium in open ocean oxygen-deficient zones. Proc. Natl. Acad. Sci. U. S. A. 111, 6888–6893.

John, S.G., 2012. Optimizing sample and spike concentrations for isotopic analysis by double-spike ICPMS. J. Anal. At. Spectrom. 27, 2123.

John, S.G., Conway, T.M., 2013. A role for scavenging in the marine biogeochemical cycling of zinc and zinc isotopes. Earth Planet. Sci. Lett. 394, 159–167.

John, S.G., Geis, R.W., Saito, M.A., Boyle, E.A., 2007. Zinc isotope fractionation during high-affinity and low-affinity zinc transport by the marine diatom *Thalassiosira oceanica*. Limnol. Oceanogr. 52, 2710–2714.

Johnston, D.T., Poulton, S.W., Tosca, N.J., O'Brian, T., Halverson, G.P., Schrag, D.P., Mavdonald, F.A., 2013. Searching for an oxygenation event in the fossiliferous Ediacaran of northwestern Canada. Chem. Geol. 326, 273–286.

Kasemann, S.A., Pogge von Strandmann, P.A.E., Prave, A.R., Fallick, A.E., Elliot, T., Hoffmann, K.-H., 2014. Continental weathering following a Cryogenian glaciation: evidence from Ca and Mg isotopes. Earth Planet. Sci. Lett. 396, 66–77.

Kasemann, S.A., Hawkesworth, C.J., Prave, A.R., Fallick, A.E., Pearson, P.N., 2005. Boron and calcium isotope composition in Neoproterozoic carbonate rocks from Namibia: evidence for extreme environmental change. Earth Planet. Sci. Lett. 231, 73–86.

Kasemann, S.A., Prave, A.R., Fallick, A.E., Hawkesworth, C.J., Hoffmann, K.-H., 2010. Neoproterozoic ice ages, boron isotopes, and ocean acidification: implications for a snowball Earth. Geology 38 (9), 775–778.

Kennedy, M.J., 1996. Stratigraphy, sedimentology, and isotopic geochemistry of Australian Neoproterozoic postglacial cap dolostones: deglaciation, $\delta^{13}C$ excursions, and carbonate precipitation. J. Sediment. Res. 66 (6), 1050–1064.

Kilner, B., Mac Niocaill, C., Brasier, M., 2005. Low-latitude glaciation in the Neoproterozoic of Oman. Geology 33, 413–416.

Kunzmann, M., Halverson, G.P., Sossi, P.A., Raub, T.D., Payne, J.L., Kirby, J., 2013. Zn isotope evidence for immediate resumption of primary productivity after snowball earth. Geology 41, 27–30.

Kunzmann, M., Halverson, G.P., Scott, C., Minarik, W.G., Wing, B.A., 2015. Geochemistry of Neoproterozoic black shales from Svalbard: implications for oceanic redox conditions spanning Cryogenian glaciations. Chem. Geol. 417, 383–393.

Lambelet, M., Rehkaemper, M., de Flierdt, T., Xue Z, van, Kreissig, K., Coles, B., Porcelli, D., Andersson, P., 2013. Isotopic analysis of Cd in the mixing zone of Siberian rivers with the Arctic Ocean-New constraints on marine Cd cycling and the isotope composition of riverine Cd. Earth Planet. Sci. Lett. 361, 64–73.

Lehmann, M.F., Sigman, D.M., McCorkle, D.C., Granger, J., Hoffmann, S., Cane, G., Brunelle, B.G., 2007. The distribution of nitrate $^{15}N/^{14}N$ in marine sediments and the impact of benthic nitrogen loss on the isotopic composition of oceanic nitrate. Geochim. Cosmochim. Acta 71, 5384–5404.

Little, S.H., Vance, D., C., W.-B., M., L.W., 2014. The oceanic mass balance of copper and zinc isotopes, investigated by analysis of their inputs, and outputs to ferromanganese oxide sediments. Geochim. Cosmochim. Acta 125, 673–693.

Little, S.H., Vance, D., McManus, J., Severmann, S., 2016. Key role of continental margin sediments in the oceanic mass balance of Zn and Zn isotopes. Geology 44, 207–210.

Maréchal, C.N., Sheppard, S.M.F., 2002. Isotopic fractionation of Cu and Zn between chloride and nitrate solutions and malachite or smithsonite at 30 °C and 50 °C. Goldschmidt Conference Abstracts (p. A484).

Maréchal, C.N., Nicolas, E., Douchet, C., Albarède, F., 2000. Abundance of zinc isotopes as a marine biogeochemical tracer. Geochem. Geophys. Geosyst. 1, 1999GC000029.

Ohnemüller, F., Prave, A.R., Fallick, A.E., Kasemann, S.A., 2014. Ocean acidification in the aftermath of the Marinoan glaciation. Geology 42 (12), 1103–1106.

Pichat, S., Douchet, C., Albarède, F., 2003. Zinc isotope variations in deep-sea carbonates from the eastern equatorial Pacific over the last 175 ka. Earth Planet. Sci. Lett. 210, 167–178.

Pons, M.-L., Fujii, T., Rosing, M., Quitté, G., Télouk, P., Albarède, F., 2013. A Zn isotope perspective on the rise of continents. Geobiology 11, 201–214.

Revels, B.N., Ohnemus, D.C., Lam, P.J., Conway, T.M., John, S.G., 2014. The isotope signature and distribution of particulate iron in the North Atlantic Ocean. Deep-Sea Res. II Top. Stud. Oceanogr. 116, 321–331.

Ripperger, S., Rehamper, M., Porcelli, D., Halliday, A., 2007. Cadmium isotope fractionation in seawater - A signature of biological activity. Earth Planet. Sci. Lett. 261, 670–684.

Sahoo, S.K., Planavsky., N.J., Kendall, B., Wang, X, Shi, X, Scott, C., Anbar, A.D., Lyons, T.W., Jiang, G. (2012) Ocean oxygenation in the wake of the Marinoan glaciation. Nature, 489, 546–549.

Schmitt, A.D., Galer, S.J.G., Abouchami, W., 2009. Mass-dependent cadmium isotopic variations in nature with emphasis on the marine environment. Earth Planet. Sci. Lett. 277, 262–272.

Shields, G.A., 2005. Neoproterozoic cap carbonates: a critical appraisal of existing models and the plumeworld hypothesis. Terra Nova 17, 299–310.

Silva-Tamayo, J.C., Naegler, T.F., Sial, A.N., Nogueira, A., Kyser, K., Riccomini, C., James, N.P., Villa, I.M., 2010. Global perturbation of the marine Ca isotopic composition in the aftermath of the Marinoan global glaciation. Precambrian Res. 373–381.

Tang, T., Love, G., Zumberge, A., Reinhard, C., Dupont, C.L., D., A., A., R., J., O., B., G., R., R., J., M.C., T.W., L., N., P., 2016. Tracking the rise of eukaryotes to ecological dominance with zinc isotopes. Goldschmidt Conference Abstracts (p. 3076).

Trindade, R.I.F., Font, E., D'Argrella Filho, M.S., Nogueira, A.C.R., Riccomini, C., 2003. Low-latitude and multiple geomagnetic reversals in the Neoproterozoic Puga cap carbonate, Amazon craton. Terra Nova 15, 441–446.

Xue, Z., Rehkämper, M., Horner, T.J., Abouchami, W., Middag, R., 2013. Cadmium isotope variations in the Southern Ocean. Earth Planet. Sci. Lett. 382, 161–172.

Yang, J., Li, Y., Liu, S., Tian, H., Chen, C., Liu, J., Shi, Y., 2015. Theoretical calculations of Cd isotope fractionation in hydrothermal fluids. Chem. Geol. 391, 74–82.

Zhao, Y., Vance, D., Abouchami, W., de Baar, H.J.W., 2013. Biogeochemical cycling of zinc and its isotopes in the Southern Ocean. Geochim. Cosmochim. Acta 125, 653–672.